Proceedings of the 2012 IEEE 12th International Conference on Bioinformatics & Bioengineering (BIBE), Larnaca, Cyprus, 11-13 November 2012

Lateral Resolution Improvement in Optical Coherence Tomography (OCT) Images

Evgenia Bousi, Costas Pitris, Member IEEE
KIOS Research Center, Department of Electrical and Computer Engineering, University of Cyprus
75 Kallipoleos St., 1678 Nicosia, Cyprus
cpitris@ucy.ac.cy

Abstract—**A novel method for lateral resolution improvement of Optical Coherence Tomography (OCT) images, which is independent of the focusing of the delivery optics and the depth of field, is presented. This method was inspired by radar range oversampling techniques. It is based on the lateral oversampling of the image and the estimation of the locations of the multiple scatterers which contribute to the signal. The information in the oversampled images is used to estimate the locations of multiple scatterers assuming each contributes a weighted portion to the detected signal, the weight determined by the location of the scatterer and the point spread function (PSF) of the system. A priori knowledge of the PSF is not required since optimization techniques can be employed to achieve the best possible enhancement of the image resolution. Preliminary results of such an approach on laterally oversampled OCT images have shown that it is possible to achieve a two-fold lateral resolution improvement. Moreover by performing deconvolution with the new improved PSF the lateral resolution can be further improved by another factor of two for a total of 4x improvement. Such improvement can be significant, especially in cases where the Numerical Aperture (NA) of the delivery optics is limited, such as, for example, in the case of ophthalmic imaging where the optics of the eye itself limit the lateral resolution.**

Keywords—Optical Coherence Tomography, oversampling, deconvolution, lateral resolution improvement

I. INTRODUCTION

Optical Coherence Tomography (OCT) imaging is continuously finding new applications in the diagnosis of disease in an ever expanding range of fields. The main advantage of OCT is its ability to acquire high resolution images (~ 1-15 μm), in a penetration depth of ~ 2-3 mm in real-time, non-invasively, and in vivo. Recent advances in speed, sensitivity, and resolution have bolstered the clinical potential of the technology. Despite the fact that penetration can only reach a few millimeters, OCT is now used for structural characterization and detection of abnormalities in many tissues. OCT technology has significantly improved over the past few years with the introduction of fast, high resolution OCT systems which are well suited for in vivo applications. However, further improvements in resolution are required for the detection of very initial stages of malignancy, as in the case of early cancer. Preliminary OCT imaging studies have not yet demonstrated the ability to differentiate subcellular morphologic changes. Sub-micron resolution would improve imaging of early neoplastic changes for cancer screening as well as permit new applications in developmental biology. It would also improve the sensitivity and specificity of diagnosis in a variety of fields including ophthalmology.

Although the axial resolution of OCT systems can be significantly improved by the use of broader bandwidth sources, the lateral resolution is fundamentally limited by the focusing of the delivery optics. There is a tradeoff between a high lateral resolution and a wide depth of field (DOF) which imposes significant limitations. Although a higher effective numerical aperture (NA) enhances the lateral resolution, it limits the DOF which is inversely proportional to the square of the effective numerical aperture (NA) of the optical system. The lateral resolution limitations become even more pronounced in the case of ophthalmic OCT imaging where the delivery of the sample beam is constrained by the optics of the eye. Furthermore, the lateral resolution of OCT systems is not constant. Only a very small range around the focal plane exhibits the optimal lateral resolution of the system, and the OCT image in the out-of-focus range is blurred laterally. Adaptive Optics (AO) or axicon lenses have been used to improve lateral resolution over large scanning depths [1,2]. It is inevitable however to suffer from aberrations when using AO. Dynamic focus and focus tracking in the sample arm have also been employed [3,4]. However, special hardware is required which limits the scanning speed and its application in real-time.

A different approach for achieving uniform lateral resolution is the use of inverse scattering algorithms [5,6]. Interferometric Synthetic Aperture Microscopy (ISAM) can achieve depth independent resolution throughout a volume where the focus is fixed at one depth [7]. The disadvantage of this method is the decrease in signal to noise ratio (SNR) away from the focus. A two-dimensional digital focusing numerical method was developed to alleviate the compromise between the lateral resolution and wide depth measurement range in OCT [8]. However this method is extremely sensitive to the phase stability of the measurements, particularly when in vivo imaging is performed and the sample movement is unavoidable.

Deconvolution methods have also been used for lateral resolution improvement by a factor of ~ 2. A non-iterative numerical method for laterally super-resolving OCT images using a depth dependent point spread function (PSF) was

developed [9]. Also Gaussian beam deconvolution for lateral resolution improvement has been employed [10]. Wiener and Lucy-Richardson OCT image restoration algorithms were implemented and compared to show that the Lucy Richardson algorithm provides a better performance [11]. Those deconvolution methods require that the PSF of the system is known. A new method which proposes an automatic point spread function estimation to deconvolve OCT images was developed, and is based on the discontinuity of information entropy [12].

In this work we present a new method for lateral resolution improvement which is independent of the focusing conditions and the depth of field, and is based on lateral oversampling and estimation of the weighted contributions of multiple scatterers. This method is inspired from radar range oversampling techniques [13]. In such methods, the images are oversampled and the information is used to estimate the locations of multiple scatterers assuming each contributes a weighted portion of the detected signal. *A priori* knowledge of the PSF is not required since optimization techniques (such as Multiple Signal Classification (MUSIC) and Range Oversampling (RETRO)) can be employed to achieve optimal enhancement of the image resolution. Preliminary results of a similar approach on laterally oversampled OCT images have shown that it is possible to achieve a two-fold lateral resolution improvement. Moreover by performing deconvolution with the new improved PSF the lateral resolution can be further improved by another factor of two for a total of 4x improvement.

II. METHODOLOGY

In OCT the lateral resolution is determined by the optics of the imaging device. The lateral resolution is defined as:

$$\Delta x = \frac{2\sqrt{\ln 2}}{\pi}\frac{\lambda_0}{NA} \qquad (1)$$

where NA is the numerical aperture of the focusing lens, and λ_0 is the center wavelength of the source. High lateral resolution can be obtained by using a large NA and focusing the beam to a small spot size. The lateral resolution is also related to the Rayleigh range z which is a measure of the depth of focus, that is:

$$z = \frac{\pi \Delta x^2}{4\lambda} \qquad (2)$$

The Rayleigh range is the distance from the focal plane to the point where the light beam diameter has increased by a factor of $\sqrt{2}$. Given the above relationship it is obvious that improving the lateral resolution produces a decrease in the depth of focus, a significant tradeoff in the design of OCT imaging devices.

In general, in OCT the transverse direction is sampled at a step of a half of Δx such that the centers of the resolution volumes are spaced by Δx/2. In the case of oversampling with a factor of L, adjacent resolution volumes overlap and are shifted by Δx/L. Therefore, signals from successive volumes will be correlated in range due to the region shared by adjacent resolution volumes. This is illustrated in Figure 1 for L= 3.

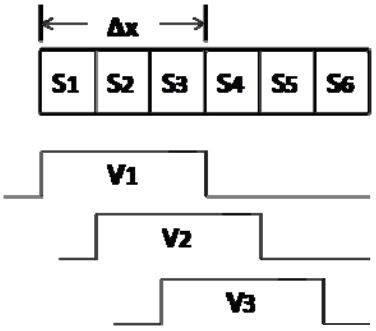

Figure 1. A schematic diagram of L=3 lateral oversampling with a rectangular PSF. Each oversampled signal Vi(t) consists of independent signals from L subvolumes (Si to SL+i-1).

We can further assume that a resolution volume with a width of Δx consists of L "subvolumes". Each subvolume has a size of Δx/L chosen to be much larger than the wavelength of light. Thus, complex signals (in-phase and quadrature-phase components) from each subvolume are independent. In other words $\langle S_i(t+\tau)S_j^*(t)\rangle = 0$ if i≠j, where $S_i(t)$ is the signal from the i-th subvolume, τ is the time lag, the asterisk is the complex conjugate, and angle brackets denote the ensemble average. Each OCT resolution volume signal $V_i(t)$ with width Δx is a weighted sum of those L independent signals ($S_i(t)$ to ($S_{L+i-1}(t)$), with the weights determined by the PSF of the system. This can be represented in the following matrix notation:

$$V(t) = QS(t) \qquad (3)$$

where $V(t) = [V_1(t) \quad V_2(t) \ldots V_L(t)]^T$ is a column vector of oversampling signals from L successively spaced resolution volumes, $S(t) = [S_1(t) \quad S_2(t) \ldots S_{2L-1}(t)]^T$ is a vector of independent signals (scatterers) at 2L-1 subvolumes within the range covered by L consecutive resolution volumes and the superscript T is the transpose. Both $V_i(t)$ and $S_i(t)$ are complex signals. Moreover, $Q = [q_1 \; q_2 \; \ldots \; q_{2L-1}]$ is a matrix of point spread functions and has a size of L×(2L-1), where q_i is a column vector of size L specifying the weights at the i-th subvolume to produce oversampled signals in V(t).

A simplified ideal, case of Eq. (2) is illustrated in Figure 1, where a rectangular PSF, and an oversampling factor L=3 are considered. Thus, the point spread function has a rectangular shape, and oversampled signals can be represented in the following form:

$$\begin{bmatrix} V_1(t) \\ V_2(t) \\ V_3(t) \end{bmatrix} = \begin{bmatrix} 1 & 1 & 1 & 0 & 0 \\ 0 & 1 & 1 & 1 & 0 \\ 0 & 0 & 1 & 1 & 1 \end{bmatrix} [S_1(t) \quad S_2(t) \quad S_3(t) \quad S_4(t) \quad S_5(t)]^T \qquad (4)$$

Each oversampled signal is simply a summation of equally weighted independent signals at those subvolumes contained in one resolution volume. For example, $V_1(t) = S_1(t) + S_2(t) +$

$S_3(t)$. In this work, the value of each element in Q is assumed to be known. The PSF would be observed from a measurement of an infinitesimally small object. Practically, the step response could be used to estimate the PSF of the system, yielding a single point approximation of the true PSF, or the PSF could be estimated from the image using optimization techniques.

Estimating the values of S(t) can yield an image with improved resolution, ideally approaching the locations of individual scatterers. By multiplying with the inverse of array Q we can extract the sub-resolution volumes $S_i(t)$:

$$S(t) = Q^{-1}V(t) \qquad (5)$$

By performing a deconvolution on the sub-resolution volumes lateral resolution will be further improved by a factor of two. The simplest image deconvolution algorithm is the "inverse filter." Because deconvolution in real space is equivalent to division in Fourier space, the inverse filtering algorithm divides the Fourier transform of an image by the Fourier transform of the PSF. Although the calculation is rapid, the utility of this method is limited by noise amplification. During division in Fourier space, small noise variations are amplified by the division operation. The result is a trade-off between blur removal and noise gain. To avoid this trade-off a number of other algorithms have been developed for image restoration. These algorithms are the so-called "constrained iterative algorithms." They work in successive cycles and, also, apply constraints on possible solutions. These constraints not only help to minimize noise or other distortions but also increase the power to restore a blurred signal. The Lucy-Richardson algorithm is used in this work for deconvolution. The Lucy-Richardson algorithm is the technique most widely used for restoring OCT images [14]. The reason for the popularity of this algorithm, which is based on a maximum likelihood implementation, is its ability to produce reconstructed images of good quality even in the presence of high noise levels [15]. The algorithm maximizes the likelihood that the resulting image, when convolved with the PSF, is an instance of the blurred image assuming Poisson noise statistics. Because it uses probabilistic error criteria, this algorithm can provide slightly better restoration than other classical techniques. Also, since it takes into account statistical fluctuations in the signal and suppresses iterations when values deviate in the vicinity of their original value, it reduces noise amplification [15].

III. Experimental Methods

The type of OCT system used in this study consisted of a superluminscent source (SLD) and a fiber optic-based Michelson interferometer. The SLD, operating at a centre wavelength $\lambda_0 \sim 1300$ nm and spectral full width half maximum (FWHM) of ~50 nm, resulted in an axial resolution of 13.5 μm. The transverse resolution of the system was 16.5 μm, the power of light incident to the sample was 8 mW, and the sensitivity of the system was measured to be 106 dB. The reference arm was scanned by translating a retro-reflector with a galvanometer. The signal from the detector was then digitized using a 16-bit 1.2 MHz data acquisition board.

To evaluate the proposed method, a phantom consisting of microspheres embedded in acrylamide gel was created. An acrylamide gel is a separation matrix commonly used in electrophoresis of biomolecules, such as proteins or DNA fragments. For the specific phantoms used in this study, a concentration 6 μm diameter spheres (Polysciences, Polybead) was chosen such that there were less than 1 sphere per resolution volume. All reagents (dH_2O, 30% acrylamide, 10% ammonium persulfate (APS)) as well as the microspheres were combined and mixed thoroughly. Tetramethylethylenediamine (TEMED) was added only when ready for polymerization to occur. The gel was allowed to polymerize for ~ 2 min.

The experimental measurement of system's PSF is done by scanning the sample arm across the edge of one element of a USAF resolution test target. This element is a high reflectivity square area and the reflectivity drops abruptly at its edge. The lateral position for a specific depth is shown in Figure 2(a). By taking the first derivative of Figure 2(a) we can find experimentally the lateral PSF of the system, at a specific depth (Figure 2(b)).

IV. Results

To evaluate the proposed method, images from the phantom consisting of 6 μm microspheres embedded in acrylamide gel were taken (Figure 3(a)). Figure 3(b) shows a single peak from line 4250 of Figure 3(a). The width of the standard OCT peak was measured at 18 μm from. After deconvolution of the standard OCT signal with the experimentally measured PSF, the width decreased to 10 μm. However, after applying the proposed method, the width also decreased to 10 μm and, after deconvolution with the new improved PSF, the width became 4.5 μm. This value is smaller than 6 μm (which is the diameter of the microsphere) since the line taken probably did not pass through the center of the sphere. In Figure 3(c), a different line (4050) is shown, where two microspheres are adjacent and are not resolvable. In the standard OCT image they appeared as a single peak. Even when deconvolution was performed on the standard OCT signal the two microspheres where still not clearly resolved. After applying the proposed method the two peaks are unmistakably separated. Despite its advantages, a limitation of the technique is an increased computational complexity. Oversampling with an oversampling factor of L requires about L times more computations than without oversampling.

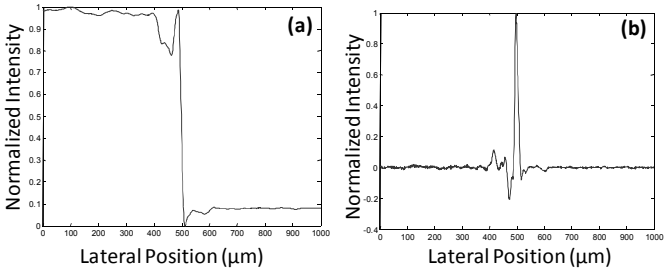

Figure 2. (a) Signal at the edge of an element of a resolution test target. (b) First derivative of (a) which gives the lateral PSF of the system.

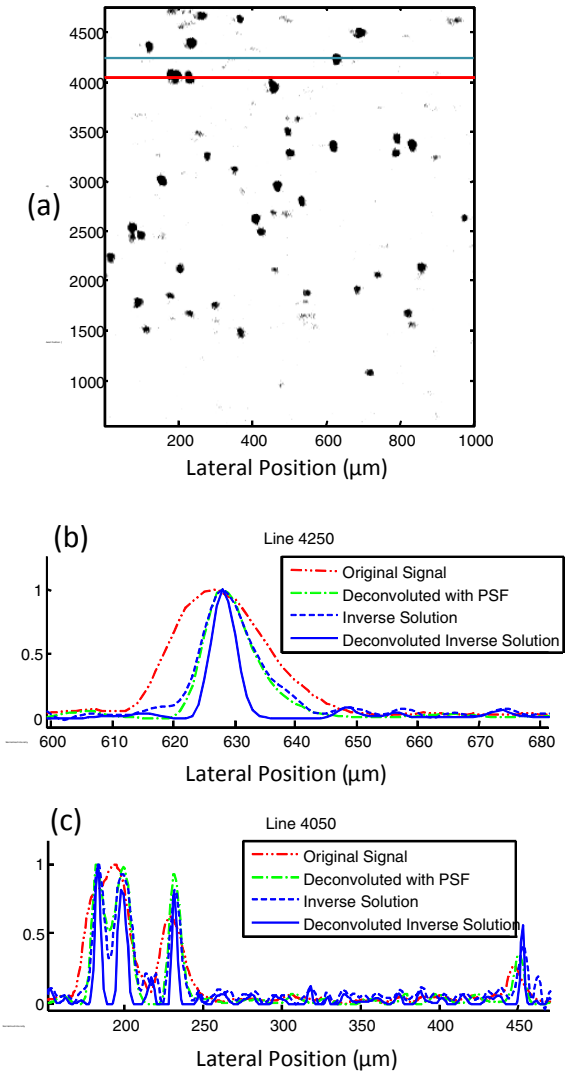

Figure 3. (a) Laterally oversampled OCT image of a phantom of 6 μm microspheres embedded in acrylamide gel, (b) Line 4250 of (a), (c) Line 4075 of (a).

V. CONCLUSION

In this work, a novel technique is presented which can improve the lateral resolution of oversampled OCT images by a factor of 4. The improvement is independent of the optics used and the depth of field. However, the lateral PSF varies with depth, and thus, for the technique to be applied as presented, the lateral PSF must be estimated for each depth. Furthermore, the PSF is also affected by the sample into which the beam is focused. Fortunately, by using optimization techniques, which are currently being implemented, the PSF does not have to be measured at all. Thus, the proposed technique can provide a tool for improving the lateral resolution of any type of OCT device and sample, including ophthalmic imaging systems where the lateral resolution is limited by the optics of the eye itself. The validation of the proposed method on ophthalmic images is planned in the near future. As usual, there is a price to pay for the benefits that are obtained. In this case, the price is paid in terms of increased computational complexity. Oversampling with an oversampling factor of L requires about L times more computations than without oversampling. But, current technology is at a point where that's just a small price to pay compared to the advantages that can be realized.

ACKNOWLEDGMENTS

This work was co-funded by the KIOS Research Center for Intelligent Systems and Networks (a University of Cyprus research center), the Republic of Cyprus, and the European Regional Development Fund of the EU.

REFERENCES

[1] B. Hermann, E. J. Fernandez, A. Unterhuber, H. Sattmann, A. F. Fercher, W. Drexler, P. M. Prieto, and P. Artal, "Adaptive-optics ultrahigh-resolution optical coherencetomography," Opt. Lett., vol. 29, no. 18, pp. 2142–2144, 2004.

[2] Z. Ding, H. Ren, Y. Zhao, J. S. Nelson, and Z. Chen, "High-resolution optical coherence tomography over a large depth range with an axicon lens," Opt. Lett., vol. 27, no. 4, pp. 243–245, Feb. 2002.

[3] Y. Wang, Y. Zhao, J. S. Nelson, Z. Chen, and R. S. Windeler, "Ultrahigh-resolution optical coherence tomography by broadband continuum generation from a photonic crystal fiber," Opt. Lett., vol. 28, no. 3, pp. 182–184, Feb. 2003.

[4] M. J. Cobb, X. Liu, and X. Li, "Continuous focus tracking for real-time optical coherence tomography," Opt. Lett., vol. 30, no. 13, pp. 1680–1682, Jul. 2005.

[5] T. S. Ralston, D. L. Marks, P. S. Carney, and S. A. Boppart, "Inverse scattering for optical coherence tomography," J. Opt. Soc. Am. A, vol. 23, no. 5, pp. 1027–1037, May 2006.

[6] T. S. Ralston, D. L. Marks, S. A. Boppart, and P. S. Carney, "Inverse scattering for high-resolution interferometric microscopy," Opt. Lett., vol. 31, no. 24, pp. 3585–3587, Dec. 2006.

[7] T. S. Ralston, D. L. Marks, P. S. Carney, and S. A. Boppart, "Interferometric synthetic aperture microscopy," Nature Physics, vol. 3, no. 2, pp. 129–134, 2007.

[8] L. Yu, B. Rao, J. Zhang, J. Su, Q. Wang, S. Guo, and Z. Chen, "Improved lateral resolution in optical coherence tomography by digital focusing using two-dimensional numerical diffraction method," Opt. Express, vol. 15, no. 12, pp. 7634–7641, Jun. 2007.

[9] Y. Yasuno, J. Sugisaka, Y. Sando, Y. Nakamura, S. Makita, M. Itoh, and T. Yatagai, "Non-iterative numerical method for laterally superresolving Fourier domain optical coherence tomography," Opt. Express, vol. 14, no. 3, pp. 1006–1020, Feb. 2006.

[10] T. S. Ralston, D. L. Marks, F. Kamalabadi, and S. A. Boppart, "Deconvolution methods for mitigation of transverse blurring in optical coherence tomography," IEEE Transactions on Image Processing, vol. 14, no. 9, pp. 1254 –1264, Sep. 2005.

[11] Y. Liu, Y. Liang, G. Mu, and X. Zhu, "Deconvolution methods for image deblurring in optical coherence tomography," J. Opt. Soc. Am. A, vol. 26, no. 1, pp. 72–77, Jan. 2009.

[12] G. Liu, S. Yousefi, Z. Zhi, and R. K. Wang, "Automatic estimation of point-spread-function for deconvoluting out-of-focus optical coherence tomographic images using information entropy-based approach," Opt. Express, vol. 19, no. 19, pp. 18135–18148, 2011.

[13] T. Y. Yu, G. Zhang, A. B. Chalamalasetti, R. J. Doviak, and D. Zrnić, "Resolution Enhancement Technique Using Range Oversampling," Journal of Atmospheric and Oceanic Technology, vol. 23, no. 2, pp. 228–240, Feb. 2006.

[14] L. B. Lucy, "An iterative technique for the rectification of observed distributions," The Astronomical Journal, vol. 79, p. 745, Jun. 1974.

[15] W. H. Richardson, "Bayesian-Based Iterative Method of Image Restoration," J. Opt. Soc. Am., vol. 62, no. 1, pp. 55–59, Jan. 1972.